Basin Research

IAS EAGE

Basin Research (2017) **29**, 798–815, doi: 10.1111/bre.12205

Gravitational deformation and inherited structural control on slope morphology in the subduction zone of north-central Chile (*ca.* 29–33°S)

Juan Becerra,* César Arriagada,* Eduardo Contreras-Reyes,† Sebastián Bascuñan,* Gregory P. De Pascale,‡ Christian Reichert,§ Juan Díaz-Naveas¶ and Natalia Cornejo†

**Laboratorio de Tectónica y Paleomagnetismo, Departamento de Geología, Facultad de Ciencias Físicas y Matemáticas, Universidad de Chile, Santiago, Chile*
†Departamento de Geofísica, Facultad de Ciencias Físicas y Matemáticas, Universidad de Chile, Santiago, Chile
‡Departamento de Geología y Centro de Excelencia en Geotermia de los Andes (CEGA), Facultad de Ciencias Físicas y Matemáticas, Universidad de Chile, Santiago, Chile
§Federal Institute and Natural Resources, Hannover, Germany
¶Pontificia Universidad Católica de Valparaíso, Valparaíso, Chile

ABSTRACT

Subduction zones provide direct insight into plate boundary deformation and by studying these areas we better understand tectonic processes and variability over time. We studied the structure of the offshore subduction zone system of the Pampean flat-slab segment (*ca.* 29–33°S) of the Chilean margin using seismic and bathymetric constraints. Here, we related and analysed the structural styles of the offshore and onshore western fore-arc. Overlying the acoustic top of the continental basement, two syn-extensional seismic sequences were recognised and correlated with onshore geological units and the Valparaíso Forearc Basin seismic sequences: (SII) Pliocene-Pleistocene and (SI) Miocene-Pliocene (Late Cretaceous (?) to Miocene-Pliocene) syn-extensional sequences. These sequences are separated by an unconformity (i.e. Valparaíso Unconformity). Seismic reflection data reveal that the eastward dipping extensional system (EI) recognised at the upper slope can be extended to the middle slope and controlled the accumulation of the older seismic package (SI). The westward dipping extensional system (EII) is essentially restricted to the middle slope. Here, EII cuts the eastward dipping extensional system (EI), preferentially parallel to the inclination of the older sequences (SI), and controlled a series of middle slope basins which are filled by the Pliocene-Pleistocene seismic sequence (SII). At the upper slope and in the western Coastal Cordillera, the SII sequence is controlled by eastward dipping faults (EII) which are the local reactivation of older extensional faults (EI). The tectonic boundary between the middle (eastern outermost forearc block) and upper continental slope (western coastal block) is a prominent system of trenchward dipping normal fault scarps (*ca.* 1 km offset) that resemble a major trenchward dipping extensional fault system. This prominent structural feature can be readily detected along the Chilean erosive margin as well as the two extensional sets (EI and EII). Evidence of slumping, thrusting, reactivated faults and mass transport deposits, were recognised in the slope domain and locally restricted to some eastern dipping faults. These features could be related to gravitational effects or slope deformation due to coseismic deformation. The regional inclination of the pre-Pliocene sequences favoured the gravitational collapse of the outermost forearc block. We propose that the structural configuration of the study area is dominantly controlled by tectonic erosion as well as the uplift of the Coastal Cordillera, which is partially controlled by pre-Pliocene architecture.

INTRODUCTION

The subduction zone system of the western Andean forearc is considered a key area to better understand continental wedge stability (e.g. Melnick & Echtler, 2006; Maksymowicz *et al.*, 2015) and subduction zone processes (Ranero *et al.*, 2006). Within the Andean subduction zone, the key factors that control and trigger tectonic processes are related to the mode of subduction (erosive or accretive); the structure of the incoming oceanic plate (e.g. Ranero *et al.*, 2006); and recently, the presence of long-lived basement architecture in the upper plate (e.g.

Correspondence: J. Becerra, Laboratorio de Tectónica y Paleomagnetismo, Departamento de Geología, Facultad de Ciencias Físicas y Matemáticas, Universidad de Chile, Plaza Ercilla #803, Santiago, Chile. E-mail: juantkd@gmail.com

Allmendinger & González, 2010; Cembrano *et al.*, 2010; Arriagada *et al.*, 2011; Farías *et al.*, 2011). By studying the areas with a particular mode or class (accretionary or erosive; e.g. Clift & Vannucchi, 2004) in the Chilean convergent margin, we can better understand how this mode influences plate boundary deformation and how this mode is controlled by the long-lived architecture. Offshore of the Pampean flat slab segment (*ca.* 27–33°S), the architecture of the marine forearc region is the result of a complex geological evolution that includes the Andean tectonic framework affected by tectonic erosive processes (e.g, von Huene *et al.*, 1997), which were enhanced by the collision and underthrusting of a major oceanic bathymetric high (The Juan Fernández Ridge or JFR). The collision of high bathymetric relief greatly influenced the tectonic evolution of the overriding plate (von Huene *et al.*, 1997). At the current position of the JFR (Fig. 1), the seismic stratigraphy and inner structure of the Valparaíso Forearc Basin displays subsidence, seaward rotation of the upper slope and thrusting in the lower and middle slope (e.g. Laursen *et al.*, 2002), produced by the collision of the JFR. In the post-collision zone between the Juan Fernández Ridge (JFR) and Chilean margin, immediately to the north of the JFR, the bathymetry and seismic reflection data (e.g. von Huene & Ranero, 2003; Kukowski & Oncken, 2006; Ranero *et al.*, 2006) show an important segmentation of the morphology of the slope into a depressed middle slope and an uplifted seaward dipping upper slope (e.g. von Huene *et al.*, 1997). This morphostructural segmentation is in agreement with a strong velocity contrast visible within the velocity depth model (*ca.* 31°S) (Contreras-Reyes *et al.*, 2014, 2015) beneath the upper continental slope (6.0–6.5 km s^{-1}), and beneath the lower and middle continental slope (3.5–5.0 km s^{-1}). This seismic framework was interpreted as an inherited volcanic-continental basement influenced by gravitational collapse as a result of frontal and basal erosion (Contreras-Reyes *et al.*, 2014). However, as well the study of co-seismic reactivation of the basement structures (e.g. Arriagada *et al.*, 2011; Farías *et al.*, 2011) of the Coastal Cordillera and the evidence of pre-Miocene compressional phases in the Arauco forearc marine basin (e.g. Becerra *et al.*, 2013) suggest that the subduction zone is influenced by Andean tectonic control. Recent studies (e.g. Arriagada *et al.*, 2011; Farías *et al.*, 2011; Contreras-Reyes *et al.*, 2014) demonstrated the control of inherited architecture on tectonic subduction zone processes, but the effects of the inherited structures remain poorly understood. We attempt to relate and analyse both onshore and offshore structural styles to constrain the structural and kinematic history of the study area, and thereby develop a better understanding for the control of the inherited architecture with the subduction erosion processes. We used swath bathymetric, seismic reflection and refraction data (Reichert *et al.*, 2002; Ranero *et al.*, 2006; Contreras-Reyes *et al.*, 2014, 2015), and western forearc geologic maps (e.g. Gana, 1991; Emparan & Pineda, 2000; Welkner *et al.*, 2006) to derive a conceptual

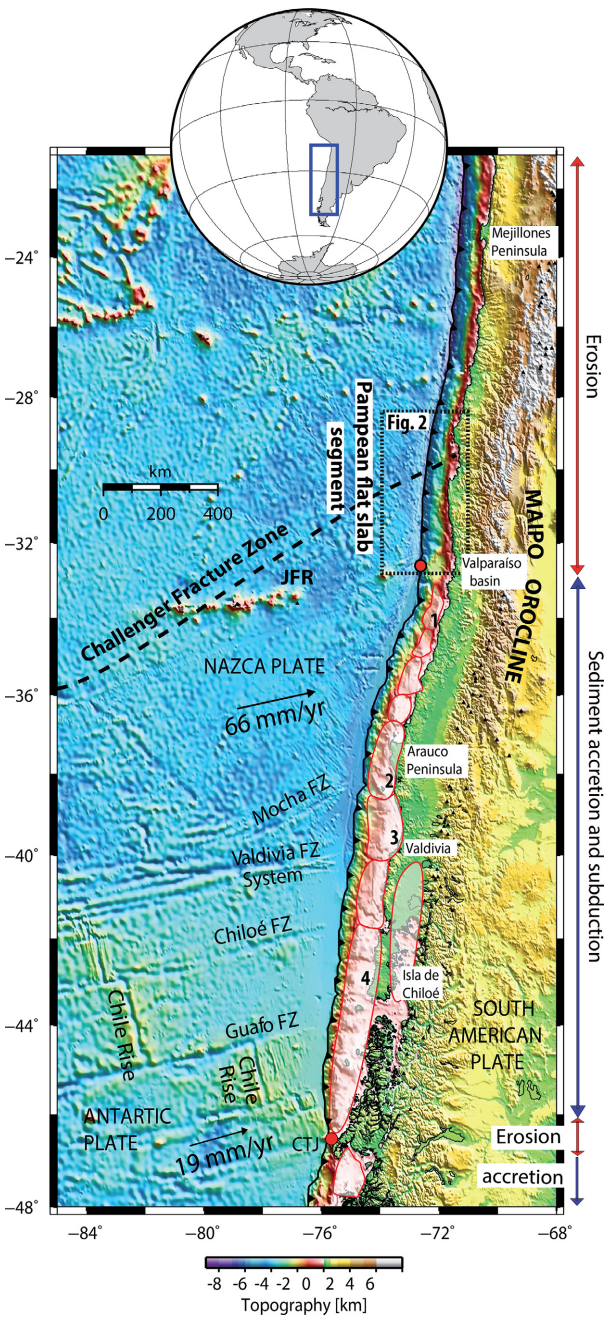

Fig. 1. Geodynamic setting of the Chilean Margin (22–48°S). Along this segment, the Chilean margin is segmented by two main oceanic features: the Juan Fernández Ridge (JFR) and the Chile Rise (CR). The erosive margin occurred immediately to the north of JFR where the trench is sediment-starved. FZ = Fracture Zone; 1 = Navidad-Algarrobo Basin; 2 = Arauco-Itata Basin; 3 = Valdivia Basin; 4 = Chiloé Basin. Red dotted box corresponds to Fig. 2. Black dotted line corresponds to Challenger Fracture Zone. CTJ: Chile Triple Junction.

2D geological and structural model of the off-Pampean flat-slab segment (*ca.* 31°S). In this study, we present new structural interpretations of the seismic reflection profiles which clearly show the marine forearc structure of the post-collision zone between the Juan Fernández Ridge (JFR) and Chilean margin, and these new results

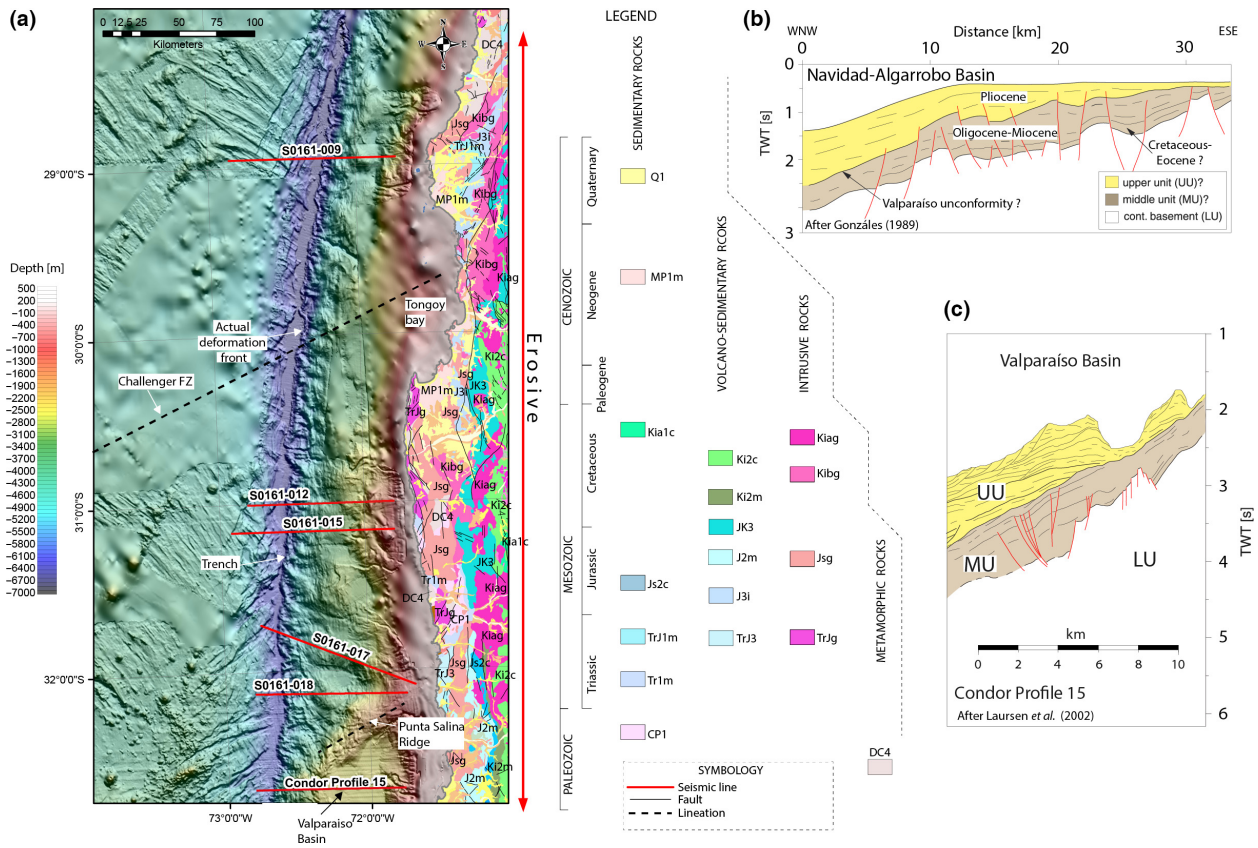

Fig. 2. Study area. (a) Swatch bathymetric data, continental structures and geological units (SERNAGEOMIN 2003). The Juan Fernández hot spot chain and Valparaíso Forearc Basin (VFB) are located immediately to the north of the study area. The VFB contains up to 3–3.5 km of Late Cenozoic strata that were deposited as a result of high subsidence and alternated compressional deformation (Laursen *et al.*, 2002). After Laursen *et al.* (2002). (b) Shelf interpretation of seismic reflection profile B, west of Navidad (*ca.* 33°50'S) (after González, 1989). After González (1989). (c) Western interpretation of seismic reflection Condor Profile 15 (*ca.* 32°40′S) (Laursen *et al.*, 2002). See (a) for location. After Laursen *et al.* (2002). The next figures show the seismic reflection data of S0161-012, S0161-018, S0161-017, S0161-015 and S0161-009.

contribute to our understanding of the nature and structure of an erosive subduction zone system.

TECTONIC SETTING

In the Chilean subduction zone, the oceanic Nazca Plate subducts beneath South America at a current rate of *ca.* 66 mm year^{-1} (Angermann *et al.*, 1999), which is slower than its mean rate of *ca.* 84 mm year^{-1} during the past *ca.* 20 Ma (Fig. 1) (DeMets *et al.*, 1994). North-Central Chile exhibits a semi-arid climate representing the transition zone between arid northern Chile and humid southern Chile climate zones (e.g. Heinze, 2003). South of the Juan Fernández Ridge (JFR) (*ca.* 33°S) and north of the Chile Rise (CR) (*ca.* 45°S), the marine forearc is characterised by a sediment-flooded trench (*ca.* 2.2 km of trench fill); an extensive and active accretionary prism (10–25 km wide); a seaward dipping slope, formed by en echelon accretionary ridges (e.g. von Huene *et al.*, 1997; Laursen *et al.*, 2002); and a wide continental shelf, about 35 km wide on average, and in some sectors greater than 60 km wide, which hosts a number of forearc marine basins (e.g. Arauco-Itata, Valdivia, Chiloe and Diego Ramirez Basins) (González, 1989). In contrast, the erosive margin north of the JFR, is characterised by a sediment starved trench; a small frontal prism; a depressed middle slope; a strong seaward dipping upper slope; a very narrow continental shelf (5–10 km wide) (von Huene *et al.*, 1997; Ranero *et al.*, 2006).

The JFR is a discontinuous hot spot chain with seamounts that acts as a barrier which interrupts the trench turbidite sediment transport to the north, separating a sediment-flooded trench south of the JFR from a sediment-starved trench north of it, and producing extensional deformation and subsidence where it collides with the margin (Fig. 2, von Huene *et al.*, 1997). The erosive process was enhanced by the collision and underthrusting of the JFR hot spot chain at about *ca.* 22 Ma at *ca.* 20°S (Yáñez *et al.*, 2001). The JFR hot spot chain migrated southward between *ca.* 22 and 10 Ma, and from about *ca.* 10 Ma to present the JFR has been underthrusting parallel to the convergence vector (Yáñez *et al.*, 2001) and adopted a quasi stationary position forming the Valparaíso Forearc Basin (Figs 1 and 2) (Laursen *et al.*, 2002). The

eastward projection of the JFR coincides with the location of the Maipo Orocline (Fig. 1) (Arriagada *et al.*, 2013); an arcuate shape that characterised the Andean margin at 33°S. The quasi stationary position since *ca.* 10 Ma of the JFR would have increased the clockwise rotation to the south of it (33–37°S) by about 10° and decreased the clockwise rotation pattern north of it (30–33°S) by about 7°–10° (Arriagada *et al.*, 2013).

The study region (Fig. 1) is located offshore of the Pampean flat slab segment, in the erosive margin between 29°S and 33°S. It is bounded to the west by the current subduction complex and to the east by the Coastal Cordillera domain. Immediately south of the study region, the Punta Salina Ridge constitutes the northern end of the Valparaíso Forearc Basin, a deepwater forearc basin which has a sedimentary thickness of 3–3.5 km (Laursen *et al.*, 2002). The Valparaiso Forearc Basin was formed by margin-wide subsidence contemporaneou with accretional deformation on the western margin (Laursen *et al.*, 2002). The Punta Salina Ridge is an area of high bathymetric relief that results from the underthrusting of the JFR beneath the continental margin (Ranero *et al.*, 2006). Laursen *et al.* (2002) observed three seismic stratigraphic units within the Valparaíso Basin (*ca.* 33°S) (Fig. 2b) that were correlated with the rocks of the Navidad-Algarrobo Basin (*ca.* 34°S) (González, 1989) (Fig. 2c): (i) the Lower Unit (LU) comprises Palaeozoic and Mesozoic rocks, forming continental basement; (ii) the Middle Unit (MU) comprises Oligocene-Miocene interbedded marine, clastic and siliciclastic sequences and with local Late Cretaceous to Eocene sediments; (iii) and the Upper Unit (UU), is composed of Late Miocene-Pliocene, marine and siliciclastic sediments. The wave base or subaerial erosion Valparaíso unconformity (Fig. 2b,c) truncates the Oligocene-Miocene sediments and constitutes the base of the Valparaíso Forearc Basin (Laursen *et al.*, 2002).

In the study area, similar to the classic model of convergent extensional margin (Aubouin *et al.*, 1985; von Huene *et al.*, 1999), the continental slope shows pervasive extensional faulting: the upper slope shows landward dipping extensional faults and the depressed middle slope is characterised by trenchward dipping extensional faults (Ranero *et al.*, 2006).

The geological units of Andean orogen present in the onshore area (Fig. 2a) are Jurassic-Cretaceous, Cretaceous, Upper Cretaceous and Cretaceous-Palaeogene igneous and stratified rocks to Late Cenozoic marine and continental sediments (SERNAGEOMIN 2003). The Andean continental basement is composed of metamorphic, intrusive and stratified rocks that range in age from Upper Palaeozoic to Jurassic (SERNAGEOMIN 2003). Regionally, the onshore area contains NS, NW and NE-trending structures (Fig. 2) mainly related to a Mesozoic extensional event (e.g. Ferrando *et al.*, 2014). Many structures affected and delimited N-NE elongated intrusive bodies and marine extensional basins (e.g. Gana, 1991; Emparan & Pineda, 2000; Welkner *et al.*, 2006). Some of these structures composed the southern segment of the long-lived Atacama Fault System (AFS) (e.g. Taylor *et al.*, 1998; Emparan & Pineda, 2006; Charrier *et al.*, 2007), called 'Romeral-La Silla del Gobernador' (Fig. 3). Nevertheless, compressional structures such as the Sistema de Falla Silla del Gobernador (Arancibia, 2004) (Fig. 2) and inverted extensional structures have been observed and associated with the Late Cretaceous-Paleogene compressive deformation event (e.g. Ferrando *et al.*, 2014).

Cenozoic basins and crustal faults are present in the Coastal Cordillera domain and well exposed near the shoreline and the Tongoy Bay (e.g. Heinze, 2003; Le Roux *et al.*, 2006) (Fig. 2). The sedimentary fill of the Cenozoic basins (e.g. Tongoy-Limari basin) is composed of Miocene-Pliocene marine sequences (MP1 m) of the Coquimbo Formation (Gana, 1991; Le Roux *et al.*, 2006), which is overlain by Plio-Pleistocene fluvial sediments (Q1) (Fig. 2), which are separated from the former by an angular unconformity (Martínez, 1979; Heinze, 2003). Immediately the south of the Tongoy bay, in the Altos de Talinay area (Fig. 3), the faults observed are predominantly normal dip-slip faults (Heinze, 2003; Saillard *et al.*, 2009, 2010) that strike sub-paralell to the coastal line (e.g. Puerto Aldea Fault, Quebrada del Teniente Fault) (Gana, 1991; Emparan & Pineda, 2006). However, some segments of this fault and other crustal structures have been interpreted as a left lateral transtensional fault (Heinze, 2003; Bourgois, 2010). The Coquimbo Formation is bounded by an eastward dipping extensional fault, called 'Puerto Aldea Fault', and the sedimentary cover contains trench-parallel extensional faults that are inclined to the east (Heinze, 2003; Emparan & Pineda, 2006).

CHARACTERISATION OF GEOLOGICAL STRUCTURES FROM SEISMIC REFLECTION

We analysed wide-angle seismic refraction and high-resolution multichannel seismic reflection data that were acquired off north-central Chile, between *ca.* 29 and 33°S, and are complemented with swath bathymetric images of the surrounding seafloor (Reichert *et al.*, 2002). The data were acquired in 2000/2001 onboard the German research vessel Sonne (Flueh & Kopp, 2002). The seismic source for the investigation was generated by a tuned set of 20 air guns with a total volume of 51.2 L (see further details of seismic processing in Reichert *et al.*, 2002). The seismic data were interpreted using 2D Move software by Midland Valley. The interpretation and characterisation of high-resolution seismic reflection lines are based on the seismic stratigraphy and kinematics of the structures and was correlated with the nearby seismic data and interpretations from the Valparaíso Forearc Basin (Laursen *et al.*, 2002). Thickness measurements presented in meters are derived from 2D depth conversion of the SO161-018 regional line (Contreras-Reyes *et al.*,

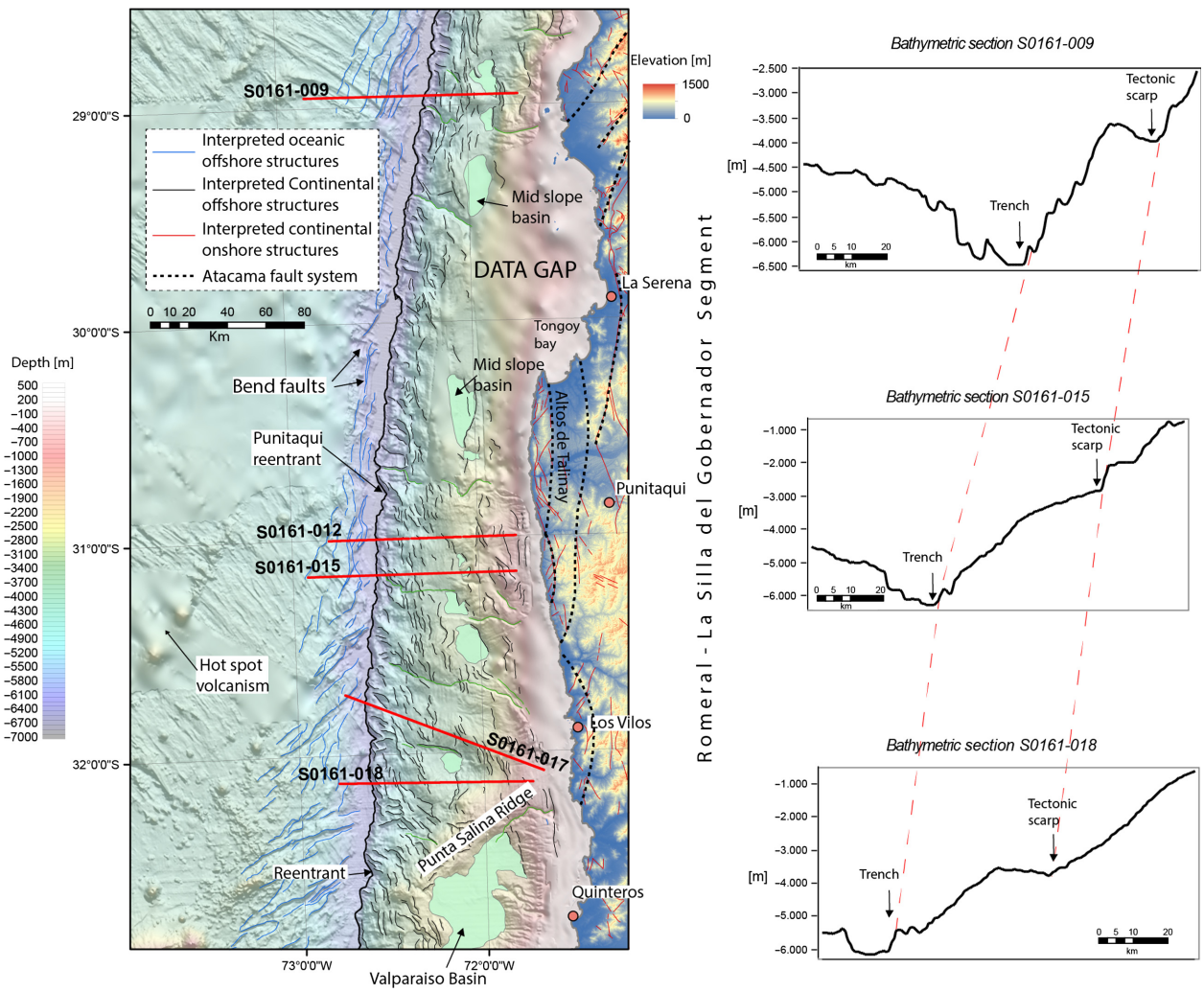

Fig. 3. Bathymetric map showing the main structural features of the study area and locations of seismic reflection lines indicated by bold red lines. Transparent area is a background hill shade from multibeam bathymetric data. Refer to the symbology for structures. The continental portion is completed with an hill shade image from SRTM data, the geological map of SERNAGEOMIN (2003) and the interpreted southern segment of the Atacama Fault System: Romeral-La Silla del Gobernador (e.g. Charrier *et al.*, 2007).

2015) as well as the bathymetric sections. Readers are referred to (Kopp, 2013 and Contreras-Reyes *et al.*, 2014, 2015) for the 2-D velocity-depth models and time to depth conversion information.

DATA DESCRIPTION

Multibeam bathymetric data show the morphology of the seafloor in this area that allows us to map structures and deformation related to the subduction zone at this local. This area is characterised by irregular seamount chain and the NW-SE trending topographic pattern of the tectonic fabric formed at the spreading center which is overprinted by NE-SW to N-S trending horst-and-graben structures caused by bending-related faulting (Fig. 3). The seafloor is covered by pelagic to hemipelagic sediments (<100 m) (e.g. Contreras-Reyes *et al.*, 2014) and the extensional faults are more frequently located in the outer rise area.

In the slope domain, the bathymetric data show a narrow continental shelf (*ca.* 8–20 km), a gently seaward inclined upper continental slope (*ca.* 3–11°) and a depressed middle slope (*ca.* 0–3°) illustrating the high segmentation of the morphology of the slope. The tectonic boundary between the upper and middle slope is well exposed, and constitutes a series of curved and straight normal fault scarps (Fig. 3). These tectonic scarps denoted a prominent extensional system that controls a series of elongated N-NW and N-NE middle slope basins (Fig. 3). From south to north, the lower slope and the frontal prism narrow from 30 to 12 km. A series of smaller and rugged reentrants indented the margin (Fig. 3). In map view, the frontal prism shows a series of ridges that are mainly arrayed en echelon in three sets (NW, N-NW and N-NE). Some of them trending parallel or obliquely to the oceanic plate bending-related faults. These morphostructural domains are cut by canyons and gullies mainly oriented W-NW, which also incise the continental shelf (Fig. 3).

Beneath the lowermost portion of the continental slope, in the subduction channel domain, remnants of oceanic plate extensional systems have been interpreted, as well as inverted tectonic geometries (?) (Figs 4b and 5b). To the west of the trench, in the outer rise region, the landward dipping faults show fault throw vertical offset of up to 1 s (TWT: Two Way Travel Time) (*ca.* 500 m; Contreras-Reyes *et al.*, 2015) (Figs 4 and 5). Turbidites and hemipelagic/pelagic sediments fill the trench, up to 0.6 s (*ca.* 300 m; Contreras-Reyes *et al.*, 2015) thick, and are imaged in a parallel configuration which is interrupted to the east by the modern deformation front (Figs 4b and 5b). The accretionary complex extends from the actual deformation front to the toe slope, and its structural style is similar to the classic compressional wedge model (Dahlen, 1990). In this domain the seismic data show thrusting, antiformal stack geometry and duplex structures with a west transport direction (Figs 4b and 5b), whereas in the modern deformation front the reflectors show an intracutaneous wedge geometry (Fig. 4b).

At the middle and upper continental slope, the relation between the growth of sedimentary sequences and faults is evident (Figs 4a and 5a) (Imber *et al.*, 2003). The sedimentary sequences are disposed on the acoustic basement and dominantly affected by extensional faults. The seismic stratigraphy and internal structure of the middle slope displays subsidence and a complex, and highly deformed area with poor image resolution. These units generally have chaotic reflectors or are acoustically void of reflections, i.e. reflection free zones (Fig. 6). However, the offset of the top of the acoustic basement suggests an extensional style composed of a domino-style fault array dipping trenchward. Here, horst-graben structures, drag folds, collapse synclines and rollover anticlines are observed (Figs 4a and 5a). The faults have similar length and offset, and show vertical fault throw differences of 0.3–0.6 s (TWT) (Figs 4a and 5a).

To the west, a prominent trenchward dipping scarp represents the natural boundary of the middle and upper slope (Figs 4a and 5a). This tectonic scarp is the seafloor expression of an important extensional system, which down-dip projection consists of one trenchward dipping fault or a set of trenchward dipping faults (Figs. 4a and 7). This structure(s) bounding the middle slope basins (Fig. 3), cuts through the entire slope fill and controlled deposition of the syn-extensional sequences. Here, the extensional depocenter of the middle slope basin is up to 1.5 s (TWT) thick and rising up vertical/fault throw differences of 1.6 s (TWT) (Fig. 4a), relative to the top of the acoustic basement. The swath bathymetric data show a prominent trenchward dipping normal scarp (*ca.* 1 km offset) related to trenchward dipping faults.

In the upper continental slope domain, the seismic reflection data show an extensional arrangement with a preferential inclination to the east. This arrangement is composed of hemigrabens, listric faults and horst-graben structures (Figs 4a and 5a). The upper slope basins show thicknesses up to 1.2 s (TWT) (Fig. 4a) and vertical fault throw differences of 0.6 s (TWT) (Fig. 4a), relative to the top of the basement. In addition, part of the upper slope morphology is controlled by partial inversion tectonics and thrusting, as indicated by a harpoon anticline (Figs 4a and 5a) and a thrust fault respectively (Fig. 4a). In the eastern and central part of the upper slope, extensional, landward dipping faults cut the basement and lower sequences, and generate drag folds and small landward dipping scarps of about 0.1 s (Figs 4a and 5a). The uplifted eastward portion of the upper slope is also an important feature visible in the seismic reflection data.

OFFSHORE GEOLOGICAL UNITS

Seismic stratigraphy was evaluated from the upper slope (coastal block) to the eastern middle slope (eastern outermost forearc block). Although in some seismic reflection lines (e.g. Figs 4 and 5), the middle slope domain is complexly deformed, and poorly imaged, high-resolution seismic lines revealed the structure and allowed for the identification of various seismic units (Figs 6 and 7). A detailed analysis allowed us to distinguish three major seismic units: the two layers within the seismic sedimentary cover (i.e. SII and SI) and the acoustic basement (Fig. 6). The sedimentary sequences are mainly bound by strong, continuous, parallel or oblique reflectors. The seismic sequences (SII and SI) are separated by an angular unconformity at the base of SII sequence. The angular unconformity can be continuously identified across the study area (Figs 5a, 6–8), and links the sub-horizontal sediments of the slope basins with the tilted underlying sediments. Despite the chaotic and free reflection character of the acoustic basement (Figs 6 and 7) at the upper portion of the basement, a discontinuous reflective pattern was mapped (Figs 6 and 7) which delimited a series of tilted blocks along the upper and middle continental slope.

Seismic sequence SI

Within the sedimentary cover, at least two syn-extensional seismic units were identified based on the configuration and character of the reflector. These syn-extensional sequences are separated by an angular unconformity. The syn-extensional I sequence (SI) is strongly controlled by extensional faults that dip generally to the east and is truncated by an unconformity. SI is deposited in onlap, tilted onlap (apparent downlap) and downlap terminations over the acoustic basement. This unit hosts wedge-shaped geometries with successions pinching out to the east (Figs 6 and 7) in both the upper and middle slope. The SI is imaged mainly as discontinuous, parallel, deformed and chaotic reflections, as well as reflection free zones. Within this unit, an unconformity is apparent in the eastern portion of the seismic lines S0161-017 and S0161-018 (Figs 5a and 6). This unconformity is also generally tilted trenchward and is deformed and predated by extensional and inverted faults (Fig. 6).

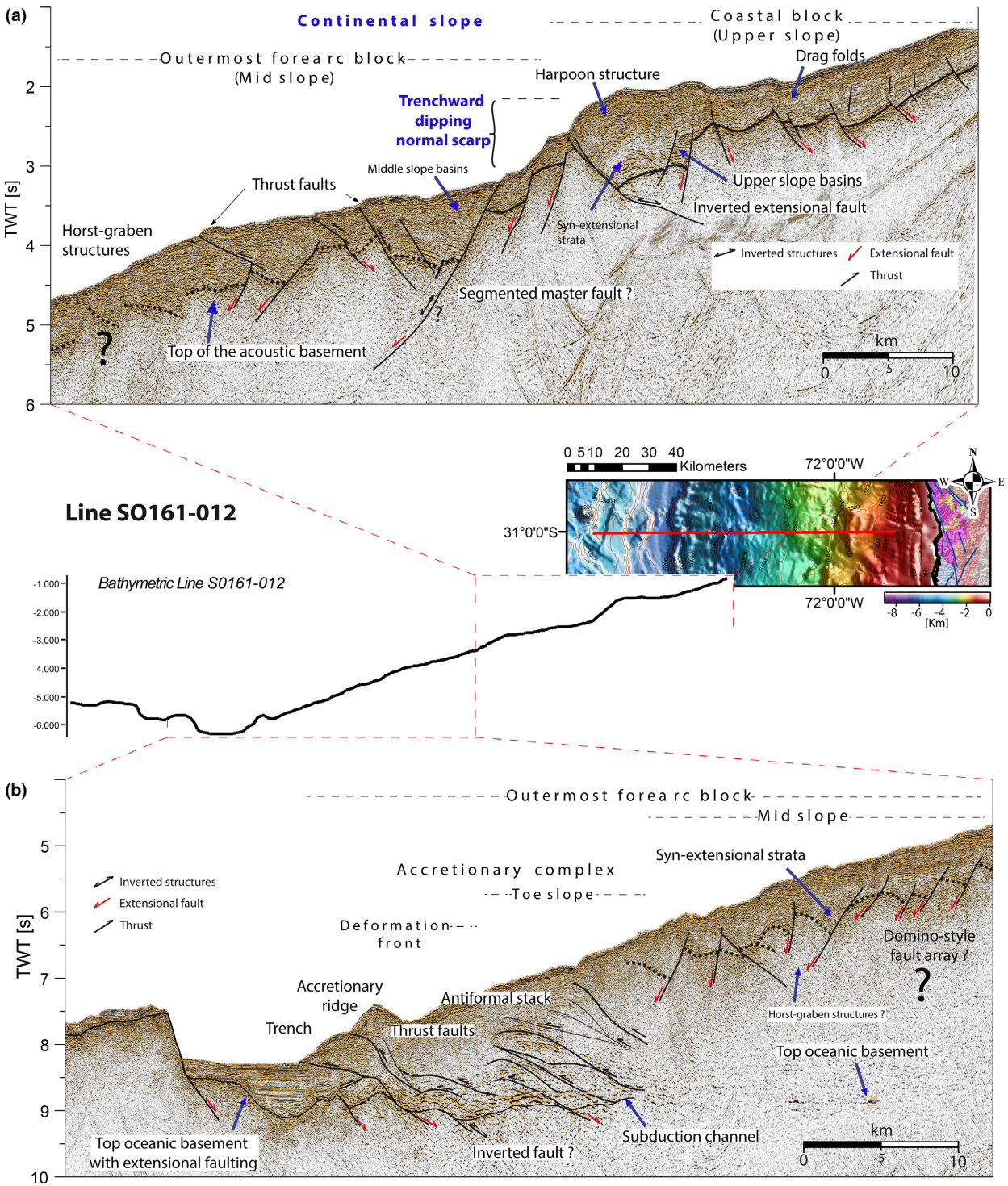

Fig. 4. S0161-012 seismic reflection line and bathymetric section illustrating the structural change between middle and upper slope. (a) Middle and upper slope domains. In his section, the structure of the middle slope is difficult to interpret due to the complexity of deformation and the low resolution of the image. In other sections, in the middle slope, two sets of extensional faults have been observed (Figs 6–8). (b) Eastern oceanic plate and middle slope domains. TWT = two way travel time. Dotted black line corresponds to the interpreted sedimentary-basement interface. After Contreras-Reyes *et al.* (2014), Ranero *et al.* (2006). Vertical scale is twice horizontal scale.

Seismic sequence SII

The syn-extensional II sequence (SII) presents a wedge geometry and overlies SI sequence in onlap and tilted onlap (apparent downlap) terminations (Fig. 6). In contrast to SI, SII is locally controlled by extensional faults that dip trenchward in the middle slope and landward in the upper slope (Figs 6 and 7). SII is imaged as sub-

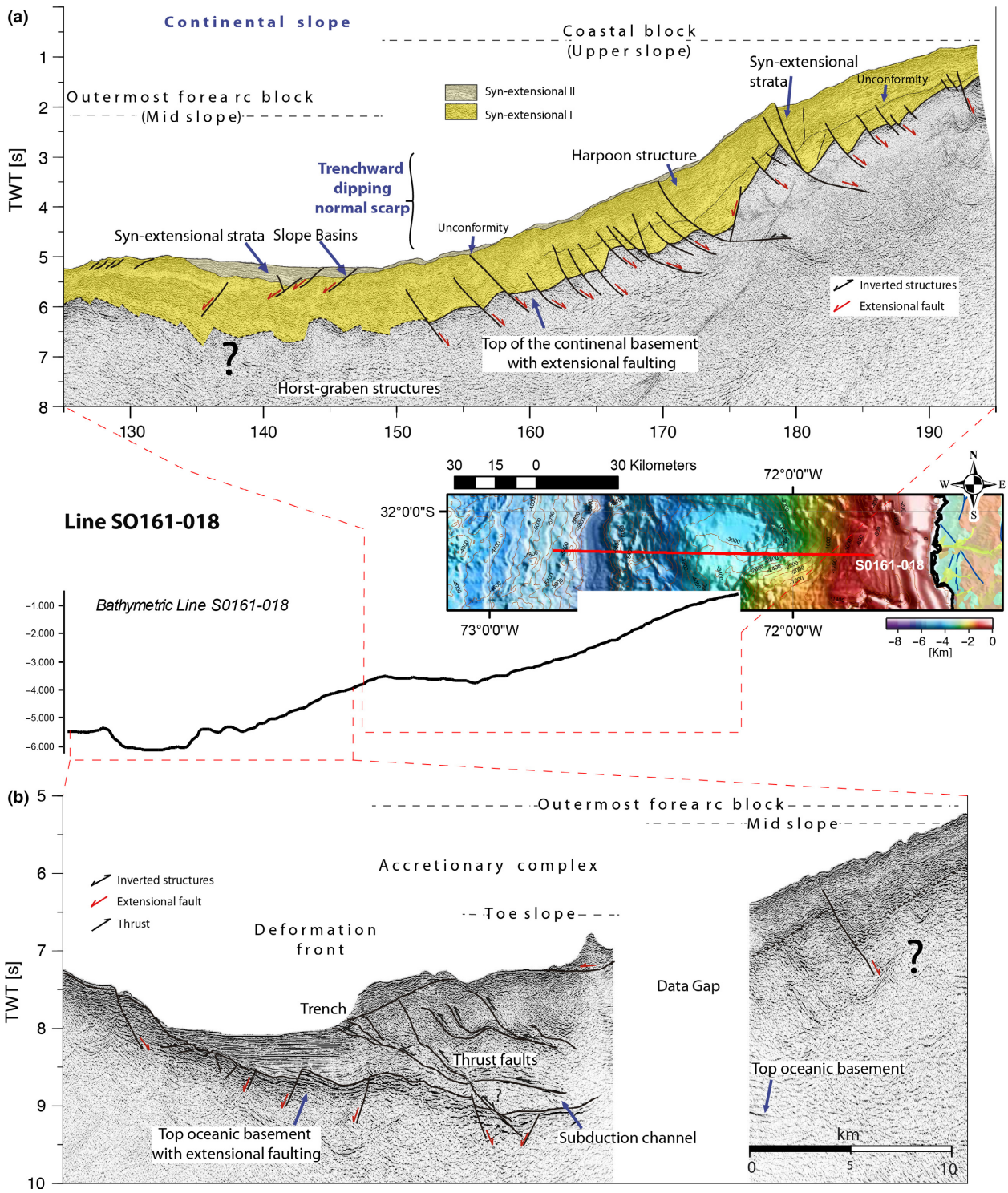

Fig. 5. S0161-018 seismic reflection line and bathymetric section. (a) Middle and upper slope domains. Similar to S0161-012, the resolution of the middle slope is poor. Dotted black line corresponds to the interpreted sedimentary-basement interface. At the middle slope two sets of extensional faults have been observed (Fig. 7). (b) Eastern oceanic plate and middle slope domains. TWT = two way travel time. After Contreras-Reyes *et al.* (2014), Ranero *et al.* (2006). Vertical scale is twice horizontal scale.

horizontal and parallel reflections (Fig. 7). This sequence filled the slope basins, where sediments onlap and thicken landward. At the upper slope the extensional faults are reactivated by older extensional faults that controlled the SI sequence. In contrast, in the middle slope the EII extensional faults cut the older EI extensional set. The reflectors are imaged as strong, parallel and laterally continuous in the upper portion. The basal section, shows discontinuous but strong reflectors, reflection free zones and small angular unconformities (Fig. 7).

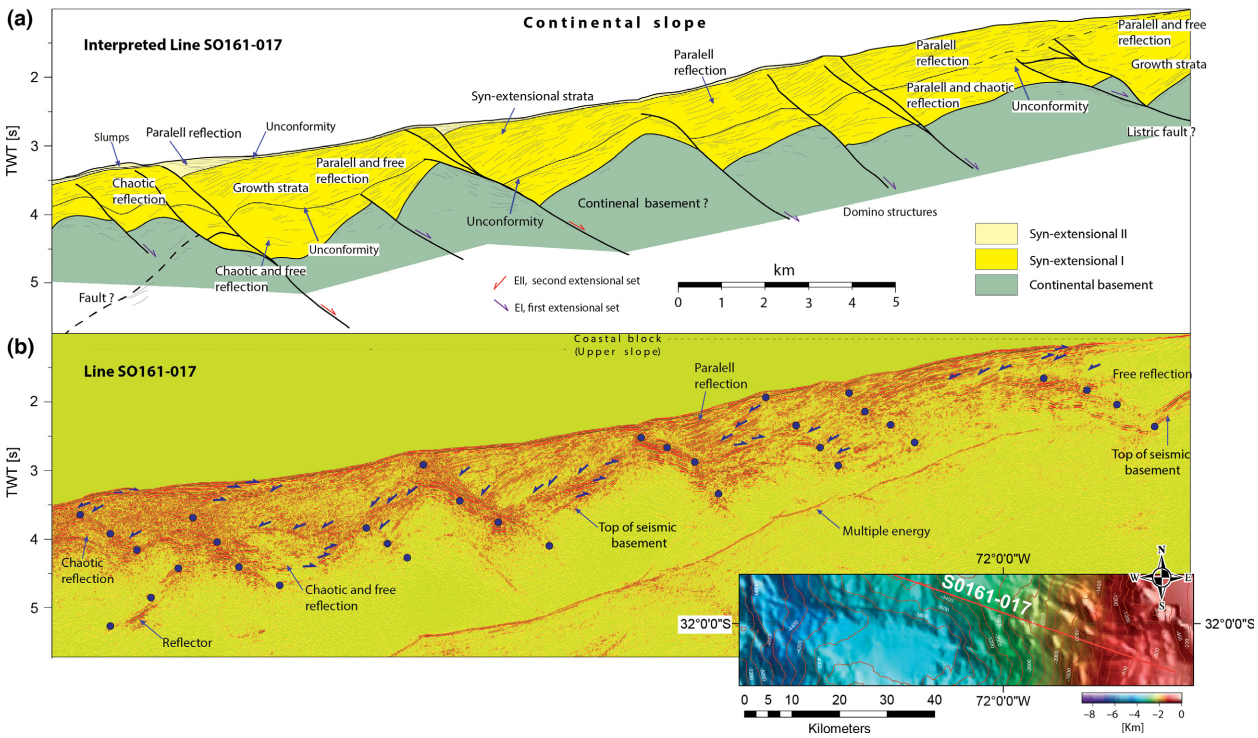

Fig. 6. Seismic stratigraphy and internal structure of the eastern segment of the S0161-017 seismic reflection line. (a) Interpreted section showing seismic character and boundary sequences. At least two syn-extensional sequences have been observed and they are separated by unconformity. (b) Post-stack time migration section with highlighted selected locations of onlaps and downlaps (purple arrows). See location in Fig. 3.Vertical scale is twice horizontal scale.

DISCUSSION

Stratigraphic correlation

Results reveal at least two extensional fault sets within the continental slope controlled two seismic sequences (SI and SII) and postdated the acoustic basement. Due to the lack of seismic stratigraphic studies and well data across the offshore study area, a correlation of the seismic stratigraphy is difficult. Stratigraphic studies, to date, have only taken place in the adjacent onshore areas (e.g. Le Roux *et al.*, 2006). However, a similar configuration of the sedimentary cover and fault patterns have been recognised in the Valparaíso (*ca.* 32°20′S–33°S) (Laursen *et al.*, 2002) and Navidad-Algarrobo forearc basins (*ca.* 33°–33°30'S) (González, 1989). The seismic interpretation of the sedimentary cover regionally reveals seismic sequences of Late Cretaceous to Eocene, Oligocene to Miocene (?) and Pliocene (?) to Holocene age (González, 1989; Laursen *et al.*, 2002). The Late Cretaceous-Eocene and Oligocene-Miocene (?) sequences were correlated with the middle unit which is separated from the upper unit of Pliocene (?)-Holocene age by the Valparaíso Unconformity (Laursen *et al.*, 2002) (Fig. 2b,c). At the southern edge of the study area, the seismic line S0161-018 (Fig. 5), is located near seismic Condor Profile 5 (Laursen *et al.*, 2002) which images the Valparaíso Unconformity. This unconformity was identified and mapped across the seismic lines of the study area (Figs 6 and 7). According to González (1989) and Laursen *et al.* (2002), the Oligocene-Miocene (?) sequences are more affected by pervasive extensional faults than the Pliocene-Holocene sequences (Fig. 2). However, it is difficult in these interpretations to identify a marked inclined pattern for extensional sets (Fig. 2). In the middle unit of the eastern portion of the Condor profile 15 (Laursen *et al.*, 2002), some structures show a preferential inclination to the east (figure 14 in Laursen *et al.*, 2002). These observations suggest that the syn-extensional sequences interpreted in this work SII and SI could be Pliocene (?)-Holocene and Oligocene-Miocene (?) age, respectively, and not older than Cretaceous-Eocene age.

The Miocene-Pliocene (MP1 m) Coquimbo Formation (Gana, 1991; SERNAGEOMIN 2003; Le Roux *et al.*, 2006) is exposed onshore, between the shoreline and the bays (Fig. 2). The Coquimbo Formation shows a tectonic contact (Puerto Aldea Fault, Fig. 2) and it onlaps the Mesozoic substratum (Gana, 1991; Heinze, 2003). The Miocene-Pliocene marine sediments are separated from the Plio-Pleistocene transgressive sequence by an angular unconformity (Heinze, 2003), which could represent a hiatus of as much as 7–8 Ma (Martínez, 1979). The Conquimbo Formation appears to gradually interfinger with the continental equivalents of the Plio-Pleistocene Limarí Formation (Gana, 1991). However, at least two sedimentary units have been identified in the onshore region of Miocene-Pliocene and Plio-Pleistocene age

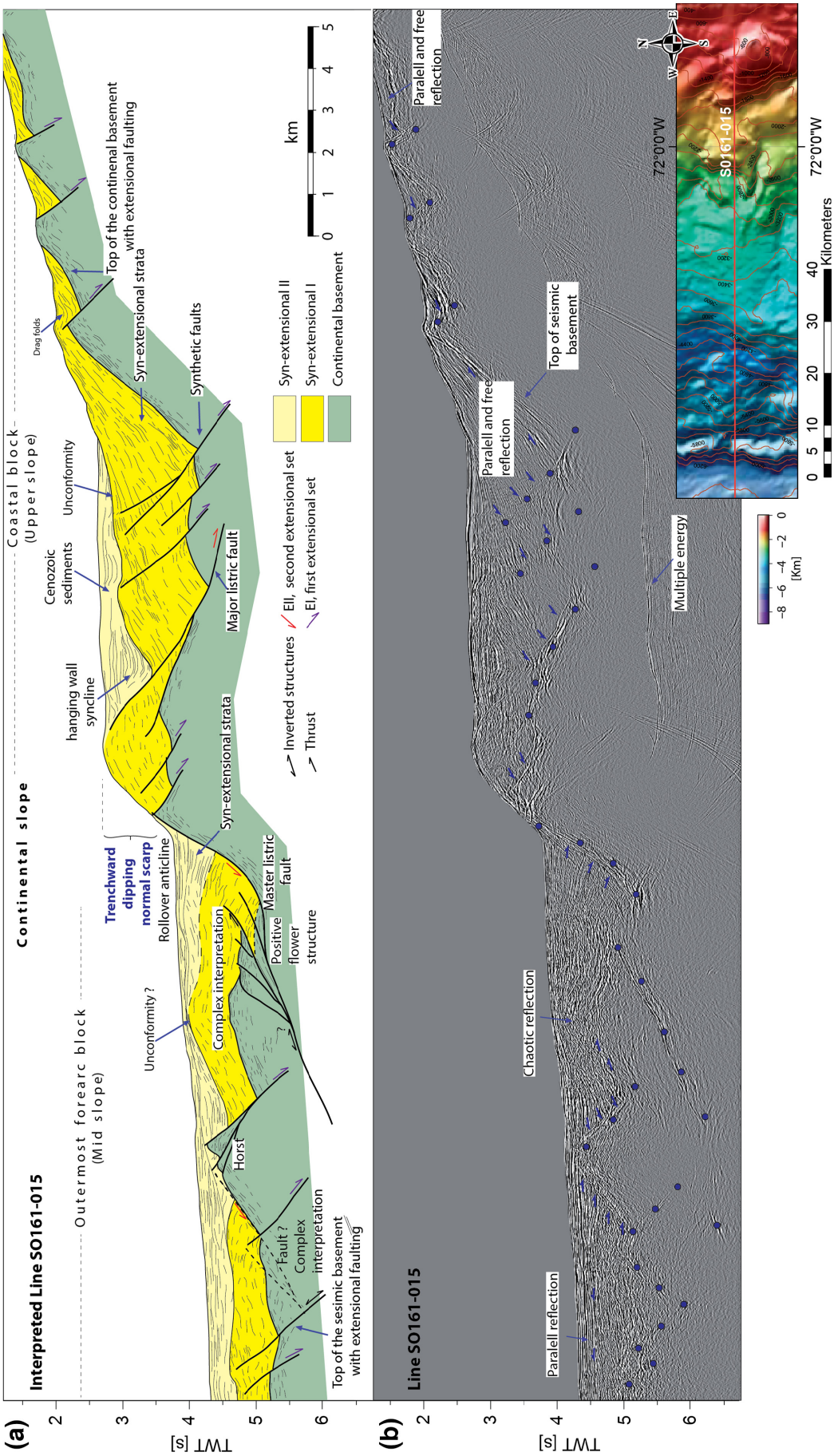

Fig. 7. Seismic stratigraphy and internal structure of the eastern outermost forearc and western coastal block from S0161-015 seismic line. See Fig. 3 for location. (a) Interpreted section. (b) Post-stack time migration section. Small angular unconformities have been mapped as continuous black line within SII package. Vertical scale is twice horizontal scale.

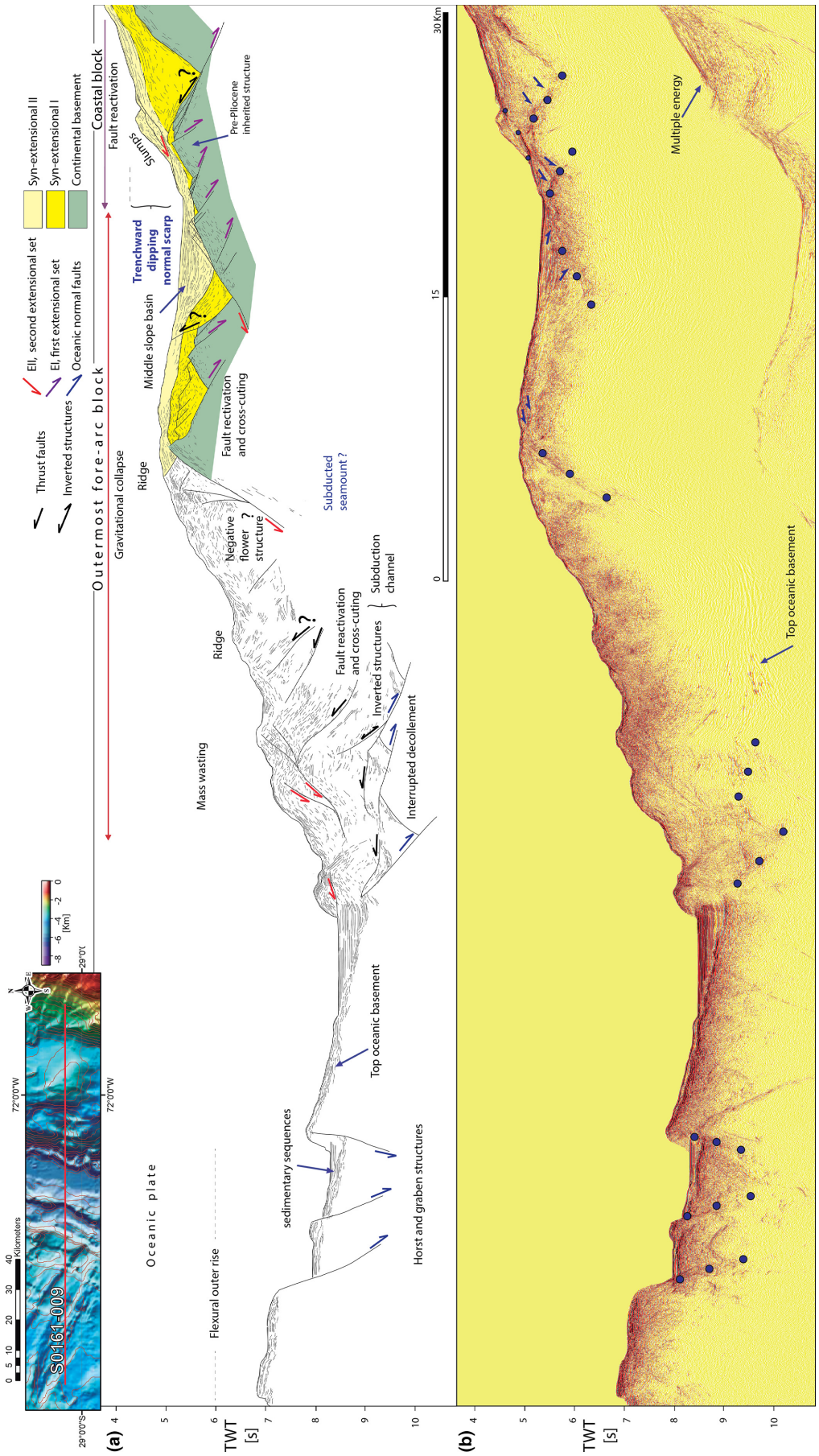

Fig. 8. (a) Regional interpretation of northernmost seismic line (S0161–009 regional) illustrating the seismic stratigraphy and structural style (geometry, kinematic and temporality of faults). (b) Poststack time migration section. Vertical scale is twice horizontal scale.

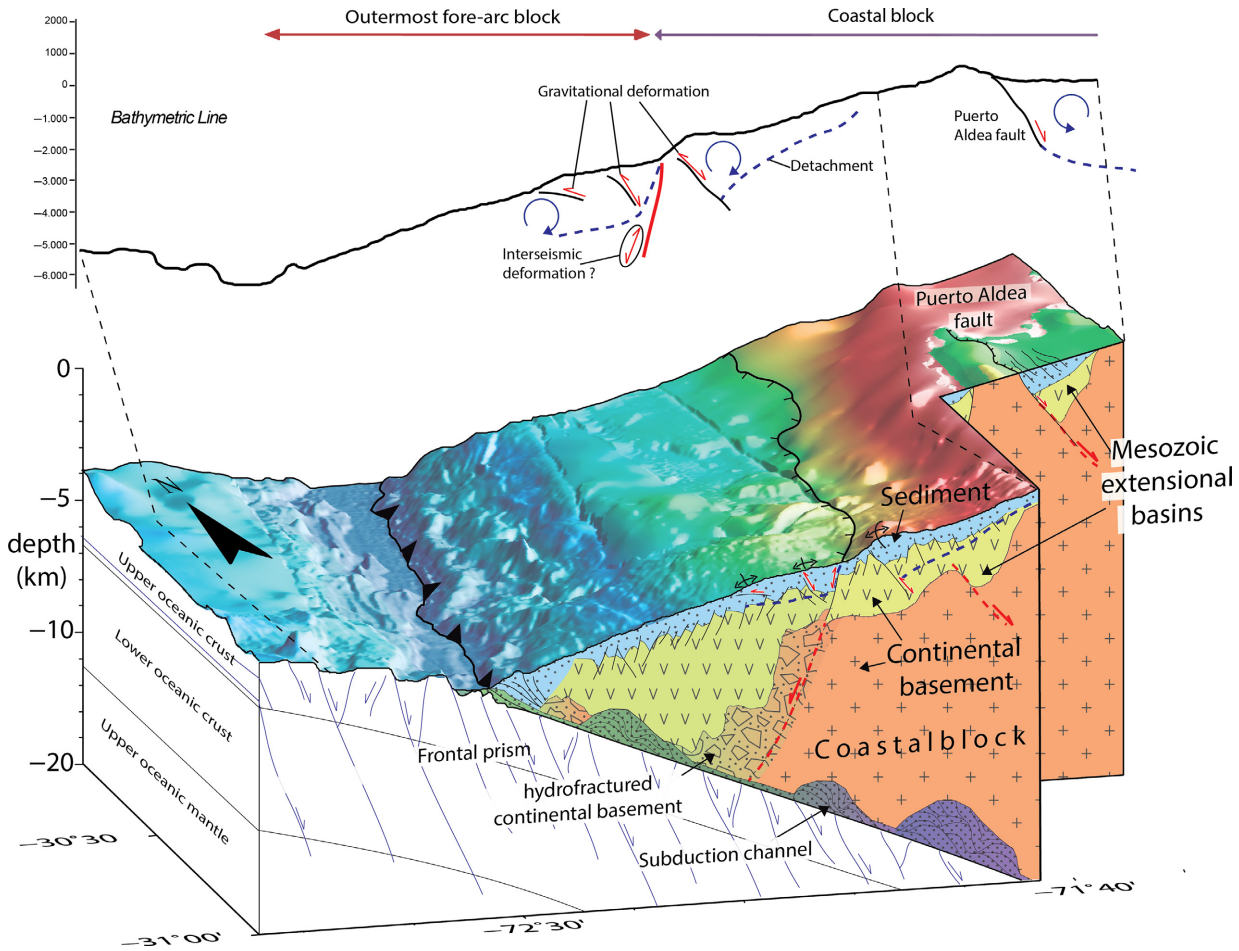

Fig. 9. Tectonic interpretation at *ca.* 31°S modified from Contreras-Reyes *et al.* (2014) and bathymetric section with highlighted locations of contractional and inverted structural features. Note the relationship between the seafloor morphology and the contractional and inverted structural features as well as the off and onshore structural style. The SII and SI sequences correspond to the sediment cover (blue light area). The acoustic basement or the continental basement is correlated with volcanic, volcano-sedimentary and sedimentary units that range in age from the Triassic to the Lower Cretaceous (yellow light area, Mesozoic extensional basin) and the Late Palaeozoic-Mesozoic metamorphic, volcanic and igneous rocks (red light area). The mass translation of rock down slope is likely induced by the large bathymetric contrast at the study area, and are probably detached (purple dotted line) along the basement-sediment interface or zones of strong velocity gradient observed in the 2-D velocity-depth model (?) (Contreras-Reyes *et al.*, 2014). The strong velocities contrast suggests the continental framework is segmented into the outermost forearc (lower and middle continental slope) and the coastal block (upper continental slope) (Contreras-Reyes *et al.*, 2014). Vertical scale approximately equal to three horizontal scale. See text for discussion.

which are separated by an angular unconformity. Although, the age of Neogene-Quaternary geological units in the onshore area do not coincide with the age of the interpreted seismic units in the Valparaíso Forearc Basin (Late Cretaceous (?)-Miocene, Middle Unit and Late Miocene-Pilocene, Upper Unit), the SI and SII sequences may be correlated with part of the onshore Miocene-Pleistocene marine sediments and the Plio-Pleistocene transgression and continental sediments respectively. In fact, SII sequences onlapping and thickening landward suggest a transgressive system. A preliminary and conservative analysis of the stratigraphy in the offshore and onshore of the study area results in Plio-Pleistocene and Late Cretaceous (?)-Pliocene (probably Miocene-Pliocene) ages for SII and SI respectively. However, the seismic stratigraphic correlation resulted in a potential range from Late Cretaceous (?) to Miocene-Pliocene for SI, and therefore it is not well constrained.

Onshore, the Mezosoic extensional basins are filled by volcanic, volcano-sedimentary and sedimentary units that range in age from the Triassic to the Lower Cretaceous (Fig. 2): Tr1 m and TrJ1 m (e.g. Canto del Agua Formation); TrJ3 (Pichidangui Formation); J3i (La Negra Formation); JK3 (Punta del Cobre Formation) and Ki2c (Quebrada Marquesa Formation) (SERNAGEOMIN 2003). These formations represent the syn-rift basin fills developed during the Mesozoic extensional event (Triassic-Lower Cretaceous, Charrier *et al.*, 2007). The basement units included in the onshore domains are probably the typical units of the Coastal Range. The inner structure of the acoustic basement shows a dominantly dip eastward extensional system that borders a series of tilted

blocks along the upper and middle slope (Figs 6–8). A similar extensional system has been identified in the onshore domain in the Andean continental basement, where extensional faults that dip essentially eastward, predated and bounded the Mesozoic volcano-sedimentary basins and the Late Palaeozoic-Mesozoic metamorphic, volcanic and plutonic rocks (e.g. Gana, 1991; Emparan & Pineda, 2000; SERNAGEOMIN 2003; Welkner *et al.*, 2006). Seismic refraction data (Contreras-Reyes *et al.*, 2014) show typical velocities of metamorphic, igneous and volcanic rocks (5.5–6.5 km s^{-1}) below the upper slope (coastal block). Similarly, at the upper continental slope, the 2D velocity depth model of (Kopp, 2013) shows zones with velocities typical of volcanic rocks (5.5–4 km s^{-1}). This volcanic velocity zone is characterised by a depocenter geometry that is suggestive of the occurrence of a Mesozoic extensional basin. With these observations, we derived a conceptual schematic section of the study area (*ca.* 31°S) (Fig. 9).

Extensional tectonics

The seismic stratigraphy and internal structure of the study area revealed at least two extensional fault sets that tectonically controlled the deposition of the marine western forearc sequences. In the outermost forearc block (from the trench to the middle slope), the younger extensional set (EII) controlled the occurrence of the SII package, and postdated the older extensional set (EI), the SI sequence and the basement (Figs 6 and 7). In the coastal block (upper slope and western Coastal Cordillera) the SII sequence is controlled by an eastward dipping set of faults (EII), some of them, corresponding to the local extensional reactivation of older extensional faults (EI) in the upper slope (Fig. 6). The younger set (EII) is dominantly composed of listric faults, segmented extensional faults and horst-graben structures. A similar structural configuration to the upper slope is identified in the southern Tongoy Bay, where the extensional faults mainly tilt eastward (Fig. 9). According to our interpretation, the EII set and SII package are related to gravitational slope collapse in the middle slope, whereas at fault geometry in the upper slope is the result of extensional faulting apparently controlled by the local extensional reactivation of an older extensional fault system (EI). Based on the kinematic features of SII, both gravitational collapse (middle slope) and the extensional faulting (upper slope) seem to be synchronous.

Along the entire continental slope (at least middle and upper slope), the landward dipping extensional system (EI) postdated the acoustic basement and strongly control the SI sequence (Figs 7 and 8). The structural configuration of the SI sequence is characterised by listric faults, horst and graben structures and an eastward dipping domino arrangement. The SI sequence is tilted towards the trench (Figs 7 and 8) and in the middle slope, the EII fault set cuts parallel to the regional inclination of SI. Thus, the SI regional inclination favoured the gravitational collapse of the outermost forearc block. We hypothesise that EI was generated in similar way to EII in the upper slope, i.e. by local reactivation of an inherited structure and/or down to the east normal fault rupture. The gravitational collapses or trenchward extensional sets which were generated synchronous with EI were probably removed by tectonic erosion enhanced by the JFR collision.

The older (EI) extensional set of faults as well as the younger (EII) extensional set which is hosted in the upper slope, could be related to different geological processes and their interaction such as: Andean extensional events (e.g. Charrier *et al.*, 2007); tectonic erosion enhanced by the collision of the JFR (e.g. von Huene & Ranero, 2003); a long-term extensional regime related to the internal shortening of the Coastal Cordillera (e.g. Delouis *et al.*, 1998; González *et al.*, 2003; Becerra *et al.*, 2013); and short-term extensional faulting during a coseismic period (e.g. Savage, 1983). The Juan Fernández hot spot track collided with the overriding South American plate some *ca.* 21 Ma ago, and reached the northern end of the study area by *ca.* 15 Ma (Yáñez *et al.*, 2001). Since then, tectonic erosion has been enhanced by the subduction of the JFR, causing crustal thinning and subsidence, which induced extensional faulting. A similar tectonic scenario is proposed by Le Roux *et al.* (2006) for the sequences of the Miocene-Pliocene Coquimbo Formation, whose sedimentation was strongly controlled by local tectonics induced by the JFR.

The extensional deformation related to EI, as well as EII in the upper slope (coastal block), was produced by buckle folding and the uplift of the coastal block (e.g. Delouis *et al.*, 1998; González *et al.*, 2003) which was driven by internal shortening (Delouis *et al.*, 1998; González *et al.*, 2003) and/or underplating (Scheuber *et al.*, 1994; Hartley *et al.*, 2000; Allmendinger & González, 2010) and, locally, the subduction of the JFR (Le Roux *et al.*, 2006), and produced an extensional rupture upward, which is strongly controlled by previous Mesozoic structures (e.g. Metcalf & Kapp, 2014). The gravitational collapse of the outermost forearc block (from the trench to the middle slope) might occur by mechanical abrasion (Adam & Reuther, 2000) and overpressured fluids hydrofracturing at the base of the continental wedge (e.g. von Huene & Ranero, 2003; Ranero *et al.*, 2008). The strong contrast between velocity zones in the refraction model suggests that the lower and middle slope (outermost forearc block) are probably fluid-saturated and disaggregated by fracturing as a consequence of frontal and basal erosion (Contreras-Reyes *et al.*, 2014).

Gravitational deformation

Gravitational deformation has played a major role in the off-Pampean flat-slab segment both due to gravitation collapse and downwarping during subduction. Within the seismic sedimentary cover, evidence of slumping (Fig. 8), reactived faults and thrusting (Figs 4a and 5a)

have been recognised in the slope domain locally restricted to some eastern dipping faults. The contractional features deformed and predated both seismic units (SI and SII) and the basement. The harpoon structure (Figs 4 and 5), a classic geometry of tectonic inversion, is associated with a landward dipping normal fault. Here, the syn-extensional sequences adjacent to the fault, are currently in a contractional state, suggesting the contractional reactivation of the previous normal fault. The harpoon geometry caused a local positive bathymetry in the upper slope (Fig. 5), suggesting the control of inversion tectonics on the slope morphology. In the western coastal block and eastern outermost forearc block, the selective reactivation of landward extensional faults as well as the presence of trenchward verging anticlines and contractional faults (Fig. 4) locally provide evidence for internal compressional stress which could be related to trenchward gravitational flows. Conversely, these contractional features could also be related to shortening during an interseismic period (discussed below). However, in the Valparaíso Forearc Basin domain, faults that ruptured with contractional focal mechanisms occurred in the upper portion of the upper slope (Contreras-Reyes *et al.*, 2015) suggesting that the gravitational deformation is an active process.

The translation of rock mass down towards the trench, induced by slope deformation, probably occur as detachments along the basement-sediment interface or along zones with strong velocity gradients as observed in the 2-D velocity-depth model (Contreras-Reyes *et al.*, 2014, 2015) (Fig. 9). To test this hypothesis, a fold-related fault analysis (e.g. Woodward *et al.*, 1989) could be performed to estimate the downdip projection of the interpreted slope structures. However, the slope tectonic induced structures are related to large-scale mass wasting processes (tectonic erosion) along this active margin, due to coseismic mass movements. This is based on the rapid deformation rates in this area with corresponding high seismic moment release. Submarine mass movements do not always have to correspond with local or regional earthquakes (e.g. Morley *et al.*, 2011; Völker *et al.*, 2011; Goldfinger *et al.*, 2012; Atwater *et al.*, 2014), however, the high interplate rates here likely contribute to development of coseismic mass transport deposits during major earthquakes.

Tectonic scarps

At the prominent trenchward normal fault scarp, some observations show contractional features; positive reactivation of the trenchward dipping master fault (Figs 4a and 7); apparent contractional state of the syn-extensional sequences adjacent to the master fault (Fig. 4a) and the apparent reverse displacement of the basement-cover interface (Fig. 7). Due to the complex geometries observed we do not rule out the presence of a strike-slip component. We speculate that these contractional features could be related to the interseismic deformation period and the strength segmentation of the continental wedge in the study area. During the interseimic period, the strain is accommodated by elastic shortening and triggers contractional faulting in the crust, whereas in the coseismic period the strain is accommodated by extension (e.g. Hyndman & Wang, 1993). For example during the Maule earthquake (Mw = 8.8) coseismic extensional structures were widely documented (e.g. Arriagada *et al.*, 2011; Farías *et al.*, 2011). The offshore bathymetry and seismic data were collected in 2000/2001, between two great subduction earthquakes: 1943 (Ms = 7.9) (Beck *et al.*, 1998) and the recent 16 Sep. 2015 (Mw = 8.3). Thus the results presented in this paper should be viewed as the structure during the interseismic period of the seismic cycle which is characterised by shortening. As such, the coastal block and the outermost forearc block are shortened and this hypothetical scenario favours contractional faulting as well as positive reactivation of normal structures. In addition, the tomographic section (Contreras-Reyes *et al.*, 2014) show that the outermost forearc block is weaker than the coastal block, and acts as a buttress. This scenario would increases the contractional strain in their tectonic limit which coincides with the prominent fault scarps. We expect an extensional reactivation of this trenchward normal scarp during the next coseismic period of deformation.

Inherited structural control on gravitational collapse

In the middle slope, the high-resolution seismic line S0161-009 (Fig. 8) shows that the trenchward dipping faults cut parallel to the inclined beds of the acoustic basement and SI seismic unit (Figs 7 and 8). The cover-basement interface, as well as the SI beds, is mainly inclined to the west. The strong regional inclination observed at these latitudes could be related to the uplift of the Coastal Cordillera.

In the onshore domain, the geological maps (e.g. Gana, 1991; Emparan & Pineda, 2000; Welkner *et al.*, 2006) yield evidence for a major Mesozoic extensional event, which is constrained by straight and curved extensional faults that are mainly inclined to the east (e.g. Puerto Aldea Fault) (Fig. 8). The resemblance between the older extensional fault set (EI) and the onshore structural styles as well as the presence of basin geometries in the tomographic sections (Contreras-Reyes *et al.*, 2014), suggests a strong control of the Mesozoic extensional architecture on the offshore structural styles (Fig. 8).

A similar configuration has been recognised along the Northern Chilean erosive margin where the continental slope is strongly segmented and hosts two extensional fault sets (e.g. von Huene & Ranero, 2003; Ranero *et al.*, 2006) with similar kinematics to the extensional sets (EI and EII) documented in this study. In addition, across the Coastal Cordillera, extensional fault sets similar to the upper slope extensional set have been recognised (e.g. González *et al.*, 2003; Allmendinger & González, 2010).

A recent study by Metcalf & Kapp (2014) suggests that the presence of inherited structure as the Atacama fault system favours the development the normal fault reactivation across the Coastal Cordillera (*ca.* 23.5°S), which is in agreement with this work. Understanding the influence of inherited structures is fundamental to improve the knowledge of the nature and structure of the subduction zone system.

CONCLUSIONS

The structural analysis of swath bathymetry and seismic reflection data allows us to constrain the structure of the post-collision zone between the JFR and the Chilean margin, immediately north of the JFR. The structural configuration, as well as the tectonic features of the study area is the result of a complex interplay between the Pre-Pliocene tectonics framework affected by tectonic erosive processes, enhanced by the collision and subduction of the JFR, as well as internal shortening and/or underplating. In the coastal block, the internal shortening and/or underplating at depth produce uplift and an upward extensional rupture, which is strongly controlled by inherited Mesozoic structures. Tectonic erosion caused the gravitational collapse of the outermost forearc block (from the trench to the middle slope).

Overlying the acoustic basement, two syn-extensional seismic sequences were identified that are spatially correlated with onshore units and the Valparaíso Basin seismic sequences: (SII) Pliocene-Pleistocene syn-extension and (SI) Miocene-Pliocene (Late Cretaceous (?) to Miocene-Pliocene) syn-extension. These sequences are separated by an erosional unconformity which is correlated with the Valparaíso Unconformity. Two extensional sets are hosted in the study area which are detectable along almost the entire erosive margin: the EI includes landward dipping extensional faults along the whole continental slope (middle and upper slope), and the EII contains collapse structures or trenchward dipping faults confined to the outermost forearc block, and controls a series of middle slope basins. At the upper slope, the EII extensional set consists of eastward dipping faults which are the local reactivation of older extensional faults (EI). The EI extensional faults strongly control the SI sequence, which is probably correlated with the onshore Miocene-Pliocene (Coquimbo Formation) geological unit. The tectonic boundary between the middle (eastern outermost forearc block) and upper continental slope (western coastal block) is a prominent system of trenchward dipping normal fault scarps (*ca.* 1 km offset) that resemble a major trenchward dipping extensional fault system.

The onshore, or western Coastal Cordillera structural style, coincides with the upper slope structural style, and both are probably controlled by long-lived weak zones like the Mesozoic extensional faults. We consider that the extensional deformation related to the EI and its regional inclination, as well as the EII at the upper slope (coastal block), were produced by the uplift and buckle folding of the coastal block. Generally, the EII fault set cuts parallel to the regional inclination of the pre-Pliocene package and the SI regional inclination favours the development of gravitational collapse of the outermost forearc block. Slumping, partial inversion tectonics and thrusting, induced by gravitational or slope deformation, are locally restricted to eastward faults. The gravitational collapse of the outermost forearc block might occur by mechanical abrasion and overpressured fluids hydrofracturing at the base of the continental wedge. Contractional features detected at the prominent trenchward normal scarp can be related to the interseismic deformation period and the buttress effect generated by the coastal block. Our new observations demonstrate the influence of inherited structures which improves our knowledge of how the subduction zone works through reactivation. Clearly, with this high-resolution baseline seismic reflection and bathymetric data set as a foundation for further analysis, by returning to this site after the next major subduction zone megathrust earthquakes and collecting new post-event data here will allow the precise quantification of coseismic and interseismic deformation in north-central Chile. We note that the 2015 Mw 8.3 Illapel Chile Earthquake likely influenced the area of our study and future fieldwork here will provide insight to co- and inter-seismic deformation along the Chilean margin.

ACKNOWLEDGEMENTS

Juan Becerra and Sebastián Bascuñan gratefully acknowledge a scholarship granted by the Chilean National Science Cooperation (CONICYT). Eduardo Contreras-Reyes thanks the Chilean National Science Foundation (FONDECYT) project 1130004. Gregory De Pascale thanks Chilean CEGA FONDAP CONICYT 15090013 for support. Midland Valley kindly provided us the Move software to perform part of the study. We also thank three anonymous reviewers for their helpful comments in earlier versions of the manuscript, and to anonymous reviewer and Dr. Elizabeth Balgord for their helpful comments in the final version of this work.

CONFLICT OF INTEREST

No conflict of interest declared.

REFERENCES

Adam, J. & Reuther, C.-D. (2000) Crustal dynamics and active fault mechanics during subduction erosion. Application of frictional wedge analysis on to the north chilean forearc. *Tectonophysics*, **321** (3), 297–325.

Allmendinger, R.W. & González, G. (2010) Invited review paper: neogene to Quaternary tectonics of the coastal Cordillera, northern Chile. *Tectonophysics*, **495** (1–2), 93–110.

Angermann, D., Klotz, J. & Reigber, C. (1999) Space-geodetic estimation of the nazca-south america euler vector. *Earth Planet. Sci. Lett.*, **171**(3), 329–334.

Arancibia, G. (2004) Mid-cretaceous crustal shortening: evidence from a regional-scale ductile shear zone in the Coastal Range of central Chile (32°S). *J. S. Am. Earth Sci.*, **17** (3), 209–226.

Arriagada, C., Arancibia, G., Cembrano, J., Martínez, F., Carrizo, D., Van Sint Jan, M., Sáez, E., González, G., Rebolledo, S., Sepúlveda, S.A., Contreras-Reyes, E., Jensen, E. & Yánez, G. (2011) Nature and tectonic significance of co-seismic structures associated with the mw 8.8 Maule earthquake, central southern Chile forearc. *J. Struct. Geol.*, **33** (5), 891–897.

Arriagada, C., Ferrando, R., Córdova, L., Morata, D. & Roperch, P. (2013) The Maipo Orocline: a first scale structural feature in the Miocene to Recent geodynamic evolution in the central Chilean Andes. *Andean Geol.*, **40**, 419–437.

Atwater, B.F., Carson, B., Griggs, G.B., Johnson, H.P. & Salmi, M.S. (2014) Rethinking turbidite paleoseismology along the Cascadia subduction zone. *Geology*. doi: 10.1130/G35902.1.

Aubouin, J., Bourgois, J., Azéma, J. & von Huene, R. (1985) Guatemala margin: a model of convergent extensional margin. *Init. Rep. Deep Sea Drilling Proj.*, **84**, 831–850.

Becerra, J., Contreras-Reyes, E. & Arriagada, C. (2013) Seismic structure and tectonics of the southern Arauco basin, south-central Chile (~ 38°S). *Tectonophysics*, **592**, 53–66.

Beck, S., Barrientos, S., Kausel, E. & Reyes, M. (1998) Source characteristics of historic earthquakes along the Central Chile subduction Askew et al zone. *J. S. Am. Earth Sci.*, **11** (2), 115–129.

Bourgois, J. (2010) A comment on "Non-steady long-term uplift rates and pleistocene marine terrace development along the andean margin of chile (31°S) inferred from 10be dating" by M. Saillard, S.R. Hall, L. Audin, D.L. Farber, G. Hérail, J. Martinod, V. Regard, R.C. Finkel. and F. Bondoux [earth planet. sci. lett. 277 (2009) 50–63]. *Earth Planet. Sci. Lett.*, **296**(3–4), 502–505.

Cembrano, J., Yánez, G., Allmendinger, R.W., González, G., Rivera, O. & Arancibia, G. (2010) Long-term geological controls on the nature and extension of earthquake rupture zones in the Chilean Andes: lessons from the 2010, mw 8.8 Maule earthquake. Gordon Conference on Rock Deformation, Tilton, NH, USA.

Charrier, R., Pinto, L. & Rodríguez, M.P. (2007) 2007. Tectono-stratigraphic evolution of the Andean orogen in Chile. In: *Geology of Chile, Special Publication* (Ed. by W. Gibbons & T. Moreno), pp. 21–116. The Geological Society, London.

Clift, P. & Vannucchi, P. (2004) Controls on tectonic accretion versus erosion in subduction zones: implications for the origin and recycling of the continental crust. *Rev. Geophys.*, **42** (2). ISSN 1944-9208. doi: 10.1029/2003RG000127.

Contreras-Reyes, E., Becerra, J., Kopp, H., Reichert, C. & Díaz-Naveas, J. (2014) Seismic structure of the north-central chilean convergent margin: subduction erosion of a paleomagmatic arc. *Geophys. Res. Lett.*, **41** (5), 1523–1529.

Contreras-Reyes, E., Ruiz Paredes, J., Becerra, J., Kopp, H., Christian, A., Reichert, C., Maksymowicz, A. & Arriagada, C. (2015) Structure and tectonics of the central Chilean margin (31°-33°S): implications for subduction erosion and shallow crustal seismicity. *Geophys. J. Int.* doi: 10.1093/gji/ggv309.

Dahlen, F.A. (1990) Critical taper model of fold-and-thrust belts and accretionary wedges. *Annu. Rev. Earth Planet. Sci.*, **18**, 55). Provided by the SAO/NASA Astrophysics Data System.

Delouis, B., Philip, H., Dorbath, L. & Cisternas, A. (1998) Recent crustal deformation in the Antofagasta region (northern chile) and the subduction process. *Geophys. J. Int.*, **132** (2), 302–338.

DeMets, C., Gordon, R.G., Argus, D.F. & Stein, S. (1994) Effect of recent revisions to the geomagnetic reversal time scale on estimates of current plate motions. *Geophys. Res. Lett.*, **21** (20), 2191–2194.

Emparan, C. & Pineda, G. (2000) Área la serena-la higuera, región de Coquimbo. Servicio Nacional de Geología y Minería, Mapas Geológicos. N° 18, escala 1:100.000. Santiago.

Emparan, C. & Pineda, G. (2006) Geología del área Andacollo-Puerto Aldea, región de Coquimbo. Servicio Nacional de Geología y Minería. Carta Geológica de Chile, Serie Geología Básica, N° 96, 85 p., 1 mapa escala 1:100.000. Santiago.

Farías, M., Comte, D., Roecker, S., Carrizo, D. & Pardo, M. (2011) Crustal extensional faulting triggered by the 2010 chilean earthquake: the pichilemu seismic sequence. *Tectonics*, **30** (6). ISSN 1944-9194. doi: 10.1029/2011TC002888.

Ferrando, R., Roperch, P., Morata, D., Arriagada, C., Ruffet, G. & Córdova, M.L.A. (2014) Paleomagnetic and magnetic fabric study of the Illapel plutonic complex, coastal range, central Chile: implications for emplacement mechanism and regional tectonic evolution during the mid-cretaceous. *J. S. Am. Earth Sci.*, **50**, 12–26.

Flueh, E.R. & Kopp, H. (2002) *Spoc (SONNE cruise so-161 leg 1 and 4), subduction processes of chile*. Geomar Rep. 102, Geomar, Kiel, Germany.

Gana, P. (1991) *Mapa geológico de la Cordillera de la Costa entre la Serena y Quebrada El Teniente, región de Coquimbo*. Servicio Nacional de Geología y Minería, Documento de Trabajo No. 3, escala 1:100.000. Santiago.

Goldfinger, C., Nelson, C.H., Morey, A.E., Johnson, J.E., Patton, J.R., Karabanov, E., Gutiérrez-Pastor, J., Eriksson, A.T., Grácia, E., Dunhill, G., Enkin, R.J., Dallimore, A. & Vallier, T. (2012) Turbidite event history-methods and implications for holocene paleoseismicity of the Cascadia subduction zone. U.S. Geological Survey Professional Paper 1661-F, **170** p.

González, E. (1989) Hydrocarbon resources in the coastal zone of chile. In: *Geology of the Andes and Its Relation to Hydrocarbon and Mineral Resources* (Ed. by G. Ericksen, *et al.*), pp. 383–404. Circum-Pac. Counc. for Energy and Miner. Resour, Houston, TX.

González, G., Cembrano, J., Carrizo, D., Macci, A. & Schneider, H. (2003) The link between forearc tectonics and Pliocene-Quaternary deformation of the Coastal Cordillera, northern Chile. *J. S. Am. Earth Sci.*, **16** (5), 321–342.

Hartley, A.J., May, G., Chong, G., Turner, P., Kape, S.J. & Jolley, E.J. (2000) Development of a continental forearc: a

cenozoic example from the Central Andes, northern Chile. *Geology*, **28** (4), 331–334.

Heinze, B. (2003) Active intraplate faulting in the forearc of North Central Chile (30°–31°S): implications from neotectonic field studies, GPS data, and elastic dislocation modelling. Scientific technical report, Geoforschungszentrum Potsdam.

von Huene, R. & Ranero, C.R. (2003) Subduction erosion and basal friction along the sediment-starved convergent margin off Antofagasta, Chile. *J. Geophys. Res. Solid Earth*, **108** (B2). ISSN 2156-2202. doi: 10.1029/2001JB001569.

von Huene, R., Corvalán, J., Flueh, E.R., Hinz, K., Korstgard, J., Ranero, C.R. & Weinrebe, W. (1997) Tectonic control of the subducting Juan Fernández Ridge on the Andean margin near Valparaíso, Chile. *Tectonics*, **16** (3), 474–488.

von Huene, R., Weinrebe, W. & Heeren, F. (1999) Subduction erosion along the north Chile margin. *J. Geodyn.*, **27** (3), 345–358.

Hyndman, R.D. & Wang, K. (1993) Thermal constraints on the zone of major thrust earthquake failure: the Cascadia subduction zone. *J. Geophys. Res. Solid Earth*, **98** (B2), 2039–2060.

Imber, J., Childs, C., Nell, P.A.R., Walsh, J.J., Hodgetts, D. & Flint, S. (2003) Hanging wall fault kinematics and footwall collapse in listric growth fault systems. *J. Struct. Geol.*, **25** (2), 197–208.

Kopp, H. (2013) Invited review paper: 2013. The control of subduction zone structural complexity and geometry on margin segmentation and seismicity. *Tectonophysics*, **589**, 1–16.

Kukowski, N. & Oncken, O. (2006) Subduction Erosion the "Normal" mode of Fore-arc Material Transfer along the Chilean Margin? In: *The Andes, Frontiers in Earth Sciences* (Ed. by O. Oncken, G. Chong, G. Franz, P. Giese, H.-J. Götze, V.A. Ramos, M.R. Strecker & P. Wigger), pp. 217–236. Springer, Berlin, Heidelberg.

Laursen, J., Scholl, D.W. & von Huene, R. (2002) Neotectonic deformation of the central Chile margin: deepwater forearc basin formation in response to hot spot ridge and seamount subduction. *Tectonics*, **21** (5), 2-1–2-27.

Le Roux, J.P., Olivares, D.M., Nielsen, S.N., Smith, N.D., Middleton, H., Fenner, J. & Ishman, S.E. (2006) Bay sedimentation as controlled by regional crustal behaviour, local tectonics and eustatic sea-level changes: coquimbo formation (Miocene-Pliocene), Bay of Tongoy, central Chile. *Sed. Geol.*, **184** (12), 133–153.

Maksymowicz, A., Tréhu, A.M., Contreras-Reyes, E. & Ruiz, S. (2015) Density-depth model of the continental wedge at the maximum slip segment of the Maule mw8.8 megathrust earthquake. *Earth Planet. Sci. Lett.*, **409**, 265–277.

Martínez, R. (1979) Hallazgo de foraminíferos miocénicos cerca de Puerto Aldea, Bahía de Tongoy, provincia de Coquimbo, Chile. *Revista Geológica de Chile*, **8**, 65–78.

Melnick, D. & Echtler, H.P. (2006) Inversion of forearc basins in south-central Chile caused by rapid glacial age trench fill. *Geology*, **34** (9), 709–712.

Metcalf, K. & Kapp, P. (2014) Along-strike variations in crustal seismicity and modern lithospheric structure of the central Andean forearc. *Geol. Soc. Am. Mem.*, **212**. doi: 10.1130/2015.1212(04).

Morley, C.K., King, R., Hillis, R., Tingay, M. & Backe, G. (2011) Deepwater fold and thrust belt classification, tectonics, structure and hydrocarbon prospectivity: a review. *Earth Sci. Rev.*, **104** (1–3), 41–91.

Ranero, C.R., vonHuene, R., Weinrebe, W. & Reichert, C. (2006) Tectonic processes along the Chile convergent margin. In: *The Andes, Frontiers in Earth Sciences* (Ed. by O. Oncken, G. Chong, G. Franz, P. Giese, H.-J. Götze, V.A. Ramos, M.R. Strecker & P. Wigger), pp. 91–121. Springer, Berlin, Heidelberg.

Ranero, C.R., Grevemeyer, I., Sahling, H., Barckhausen, U., Hensen, C., Wallmann, K., Weinrebe, W., Vannucchi, P., von Huene, R. & McIntosh, K. (2008) Hydrogeological system of erosional convergent margins and its influence on tectonics and interplate seismogenesis. *Geochem. Geophys. Geosyst.*, **9** (3). ISSN 1525-2027. doi: 10.1029/2007GC001679.

Reichert, C., Schreckenberger, B., and the SPOC Team. (2002) Fahrtbericht SONNE-Fahrt so161 leg 2y3 spoc, subduktions prozesse vor chile-bmbf forschungsvorhaben 03g0161a-Valparaiso 16.10.2001- Valparaiso 29.11.2001. fuer Geowis. und Rohsto_e. Bundesanst, Hannover, Germany, 8.

Saillard, M., Hall, S.R., Audin, L., Farber, D.L., Hérail, G., Martinod, J., Regard, V., Finkel, R.C. & Bondoux, F. (2009) Non-steady long-term uplift rates and Pleistocene marine terrace development along the Andean margin of Chile (31°S) inferred from 10be dating. *Earth Planet. Sci. Lett.*, **277** (1–2), 50–63.

Saillard, M., Hall, S.R., Audin, L., Farber, D.L., Martinod, J., Regard, V., Pedoja, K. & Hérail, G. (2010) Reply to a comment on "Non-steady long-term uplift rates and Pleistocene marine terrace development along the andean margin of chile (31°S) inferred from 10be dating" by m. Saillard, S. R. Hall, L. Audin, D. L. Farber, G. Hérail, J. Martinod, V. Regard, R. C. Finkel and F. Bondoux [earth planet. sci. lett. 277(2009) 50–63]. *Earth Planet. Sci. Lett.*, **296**(3–4):506–509.

Savage, J.C. (1983) A dislocation model of strain accumulation and release at a subduction zone. *J. Geophys. Res. Solid Earth*, **88** (B6), 4984–4996.

Scheuber, E., Bogdanic, T., Jensen, A. & Reutter, K.-J. (1994) Tectonic Development of the North Chilean Andes in Relation to Plate Convergence and Magmatism Since the Jurassic. In: *Tectonics of the Southern Central Andes* (Ed. by K.-J. Reutter, E. Scheuber & P.J. Wigger), pp. 121–139. Springer, Berlin, Heidelberg.

SERNAGEOMIN (2003) *Geologic map of Chile: Digital version, scale 1:1.000.000*. Servicio Nacional de Geología y Minería, Santiago, Chile.

Taylor, G.K., Grocott, J., Pope, A. & Randall, D.E. (1998) Mesozoic fault systems, deformation and fault block rotation in the Andean forearc: a crustal scale strike-slip duplex in the Coastal Cordillera of northern Chile. *Tectonophysics*, **299** (1–3), 93–109.

Völker, D., Scholz, F. & Geersen, J. (2011) Analysis of submarine landsliding in the rupture area of the 27 February 2010 maule earthquake, Central Chile. *Mar. Geol.*, **288** (1–4), 79–89.

Welkner, D., Arévalo, C. & Godoy, E. (2006) Geología del área Freirina-El Morado, región de Atacama. Servicio Nacional de Geología y Minería, pages Serie Geología Básica 100: 50 p., 1 mapa escala 1:100.000. Santiago.

Woodward, N.B., Boyer, S.E. & Suppe, J. (1989) *Balanced Geological Cross-Sections, in balanced geological cross-sections: An essential technique in geological research and exploration*. American Geophysical Union, Washington, DC.

Yáñez, G.A., Ranero, C.R., von Huene, R. & Díaz, J. (2001) Magnetic anomaly interpretation across the southern central Andes (32–34°S): the role of the Juan Fernández ridge in the Late Tertiary evolution of the margin. *J. Geophys. Res. Solid Earth*, **106** (B4), 6325–6345.

Manuscript received 12 January 2015; In revised form 3 May 2016; Manuscript accepted 10 May 2016.